

Polymer Chemistry

Accepted Manuscript



This is an *Accepted Manuscript*, which has been through the Royal Society of Chemistry peer review process and has been accepted for publication.

Accepted Manuscripts are published online shortly after acceptance, before technical editing, formatting and proof reading. Using this free service, authors can make their results available to the community, in citable form, before we publish the edited article. We will replace this *Accepted Manuscript* with the edited and formatted *Advance Article* as soon as it is available.

You can find more information about *Accepted Manuscripts* in the [Information for Authors](#).

Please note that technical editing may introduce minor changes to the text and/or graphics, which may alter content. The journal's standard [Terms & Conditions](#) and the [Ethical guidelines](#) still apply. In no event shall the Royal Society of Chemistry be held responsible for any errors or omissions in this *Accepted Manuscript* or any consequences arising from the use of any information it contains.

Crystalline Structures and Crystallization Behaviors of Poly(L-lactide) in Poly(L-lactide)/Graphene Nanosheets Composites

Jingqing Li¹, Peitao Xiao¹, Hongfei Li^{*2}, Yao Zhang¹, Feifei Xue¹, Baojing Luo¹,
Shaoyong Huang³, Yingrui Shang¹, Huiying Wen⁴, Jesper de Claville
Christiansen⁵, Donghong Yu⁶, Shichun Jiang^{*1}

¹School of Materials Science and Engineering, Tianjin University, Tianjin 300072, P.
R. China

²State Key Laboratory of Polymer Physics and Chemistry, Changchun Institute of
Applied Chemistry, Chinese Academy of Sciences, Changchun 130022, P. R. China

³Key Laboratory of Polymer Eco-materials, Changchun Institute of Applied
Chemistry, Chinese Academy of Sciences, Changchun 130022, P. R. China

⁴College of Engineering and Technology, Northeast Forestry University, Harbin
150040, P. R. China

⁵Department of Mechanical and Manufacturing Engineering, Aalborg University,
DK-9220, Aalborg, Denmark

⁶Department of Biotechnology, Chemistry, and Environmental Engineering, Aalborg
University, DK-9000, Aalborg, Denmark

* Corresponding authors: hfli@ciac.ac.jl, scjiang@tju.edu.cn

Abstract

Poly(L-lactide) (PLLA)/Graphene Nanosheets (GNSs) composite and pure PLLA were prepared by solution blending method. Crystalline structures and crystallization behaviors of PLLA in the composite were investigated by XRD, POM, SAXS, and DSC. It was found that α' form PLLA formation seemed to be more preferred than α form PLLA formation in PLLA/GNSs composite at crystallization temperatures T_c s within α' - α crystal formation transition region due to GNSs existence, resulting in an obvious shift of α' - α crystal formation transition of PLLA in PLLA/GNSs towards high T_c s comparing with that of pure PLLA. At T_c s below α' - α crystal formation transition, the formed α' crystal turned to be more imperfect due to GNSs addition, while at T_c s above α' - α crystal formation transition, the crystal structure of α form PLLA was not affected by GNSs. Further POM observations at high T_c s with only α crystal formed showed that PLLA spherulites were well formed in both PLLA/GNSs and pure PLLA, however with very different crystallization kinetics while isothermally crystallizing at different T_c s. The PLLA crystallization process of PLLA in PLLA/GNSs was accelerated by GNSs with both the nucleation rate and spherulite growth rate increased mainly because of the increasing segmental mobility of PLLA chains due to GNSs addition; whereas, GNSs showed no observable influence on the determined zero growth temperature T_{zg} of α form PLLA and the T_{zg} was estimated lower than the equilibrium melting point of PLLA, indicating that the crystal growth of PLLA is mediated by a transient mesophase with the transition temperature of T_{zg} between the mesophase and melt not influenced by GNSs in PLLA. Synchrotron on-line SAXS results revealed that the long periods of PLLA in PLLA/GNSs composite isothermally crystallized at different T_c s are much smaller than those in pure PLLA. The GNSs is helpful to form more perfect recrystallized α form PLLA after the α' form PLLA is melted with increasing T_c s. The presence of GNSs resulted in imperfect α form PLLA from melt directly when isothermally crystallized at different T_c s within the temperature range of α' - α crystal formation transition.

Keywords

Poly(L-lactide), Graphene Nanosheets, Crystallization Behaviors, Crystalline Structure, α' - α crystal formation transition

1. Introduction

Poly(L-lactide) (PLLA) is one of the most important friendly environmental semi-crystalline polymeric materials which can be produced from renewable carbon

sources. Many researchers believed that PLLA is a powerful potential alternative for fossil-based polymers. Nowadays, PLLA has already been successfully industrialized and found possessing excellent mechanical performances and good biocompatibility, which made it possible for PLLA to be widely used in different fields ^[1-17]. For example, it has been successfully used in biodegradable and biocompatible packings and artificial scaffold and drug delivery carriers ^[1, 2]. However, the demands in some special fields are complex and it is difficult for pure PLLA to meet them all. As known, polyethylene can be melt-blown into agricultural films and find remarkable applications in agricultural crop production; whereas, low melt strength and low crystallization rate of biodegradable PLLA during melt-blowing process limit its applications in agriculture while comparing with polyethylene. Modifications of PLLA would be needed to meet with such requirements as well as those in other applications. Since the properties and applications of PLLA or modified PLLA-based materials are closely related to their structural characteristics, the crystal and crystalline structures, crystallization behaviors and crystallization mechanism of the materials have attracted attention of many researchers ^[3, 12-17] seeking for efficient modification methods for PLLA.

In PLLA, three main crystal forms can usually be formed, including α , β , and γ crystal forms. Among them, α form is orthorhombic and has a 10_3 helical chain conformation and it is the most stable one and can usually be prepared from melt or solution ^[8, 12]. As reported by many researchers ^[7, 12, and 15-17], α form has a disordered form of α' form which has been experimentally proved as a new crystalline different from α form in terms of disordered helical chain conformation and disordered chain packing mode ^[5, 15, 18] and usually can be obtained at relatively low crystallization temperature T_c from PLLA melt. β form is an orthorhombic unit cell with 3_1 helical conformation and can be obtained by stretching at a high drawing rate and high drawing temperature ^[3, 8]. γ form can be formed at slightly low temperature when PLLA crystallizes epitaxially on hexamethylbenzene ^[17]. Here it should be noticed that formation of α form from melt is dependent on T_c ^[12] and there is an existence of crystal formation transition from α crystal to α' crystal with decreasing T_c , which is called “ α' - α crystal formation transition” in this work. That is, PLLA can crystallize as α form when T_c is higher than 120 °C, while α' form would appear together with α form if T_c is controlled between 120 °C and 90 °C. And when T_c is lower than 90 °C, only α' form was obtained and α form was not detectable. If α' form PLLA is further increased to high temperatures, it can transform into α form PLLA by melting and

re-crystallizing^[12], which is called “ α' - α crystal transition” in this work. In the past years, many researchers and groups have focused on the crystal structure variations together with the crystallization behaviors of PLLA after different modifications by tuning the processing conditions^[1, 3-5], blending with other materials^[6-8], and adding different kinds of additives to PLLA^[9-11]. And the resulting structure and properties of the modified PLLA-based materials were investigated^[1, 4-11] for further understanding to the crystallization behaviors and even the crystallization mechanism of PLLA influenced by different factors.

It has been revealed that the lamellar orientation, long periods, and crystal structures of PLLA are dependent on shear conditions, including temperatures, shear rates, and shear strains^[1, 5]. For example, Huang *et al.*^[5] found that melt shear flow favors formation of α form more than α' form, resulting in a shift of α' - α crystal formation transition towards low temperatures, and melt shear can remarkably shorten inducement time and act as nucleation agent^[5]. Wang *et al.*^[19] found that the applied melt shear could enhance nucleus density but could not affect the spherulite growth rates of PLLA. This indicated that the crystalline structure and crystallization kinetics of PLLA can be tuned by processing conditions which can obviously affect the states and behaviors of the PLLA molecular chains before and while they enter the crystals.

By blending with other materials^[6-8], the structures and properties of PLLA can also be tuned. Pan^[6] reported that crystallization of PLLA could be hindered by the dilution effect of poly(D, L-lactide) (PDLLA) miscible with PLLA at all compositions. This dilution effect of PDLLA is different from the acceleration effect of melt shear reported by Huang *et al.*^[5], but formation of α form crystal was also favored and the critical temperatures of α' - α crystal formation transition decreases from those of pure PLLA. Pan^[6] proposed that formation of α' form crystals of PLLA is kinetically preferential, while that of the thermally stable α form crystals is thermodynamically favored. From this point of view, PDLLA and melt shear mainly affected PLLA crystallization kinetically and thermodynamically, respectively. Lai^[8] blended PLLA with 1,3:2,4-Dibenzylidene-D-sorbitol (DBS) and found that DBS favored the order and regular α form of PLLA as well as melt shear and dilution effect of PDLLA and at lower temperatures α form crystal formed more, which made the α' - α crystal formation transition temperature of PLLA shift towards lower temperature as more DBS was added. It was proposed that DBS molecules are stacked together through π - π interaction to form a strand with PLLA molecules by hydrogen bonding and this makes PLLA have a more regular structure but its equilibrium melting point and

glass-transition temperature were not significantly changed. Similarly to the effect of PDLA, DBS also decreased the crystallization rate of PLLA though more DBS may act as nucleation agent, which was attributed to the variation of crystal structure of PLLA by the authors. This explanation to the decrease of PLLA crystallization rate is different from those reported by Pan ^[6] in PLLA/PDLA.

Kinds of different additives are always used as nucleation agent or other functional additives of polymeric materials, especially some typical nano additives developed in recent years ^[9-11, 20-48]. The additives include exfoliated graphite ^[9], carbon nanotubes ^[11, 25-34] including single wall carbon nanotube ^[29-33] and multi-walled carbon nanotubes ^[11, 34], graphite oxide ^[38-40], graphene nanosheets (GNSs) ^[10, 20-24], montmorillonite ^[35-37], layered silicates ^[41], and other additives ^[42-45]. It has been found that many of these additives can be used to tune the mechanical performances of the filled polymeric composites by tuning their crystallization behaviors and crystalline structures, including crystallization kinetics and crystalline morphology ^[10, 26-32, 34-37, and 41-43]. And many of them have been used to modify the properties and structures of PLLA ^[9-11]. For example, Kim ^[9] reported that addition of exfoliated graphite to PLLA matrix to form nanocomposites could enhance the material's thermal stability, mechanical modulus, and electrical conductivity. Villmow ^[11] dispersed multi-walled carbon nanotubes in a poly(lactic acid) matrix by tuning twin-screw extrusion conditions and found an electrical percolation threshold was reached below 0.5 wt% MWNT content. With thermally reduced graphene oxide (tr-GO) as initiator, Yang ^[49] prepared PLLA/tr-GO composites via *in situ* ring-opening polymerization of lactide and found the thermal stability, crystallization rate, and electrical conductivity of the materials were increased. Wang ^[39, 50] reported that graphene oxide (GO) could accelerate the nonisothermal cold crystallization and isothermal crystallization nucleation density of PLLA, indicating that GO may act as a nucleating agent for PLLA, while the crystallization mechanism and crystal structure remained unchanged at $T_c=130$ °C. Chen ^[40] found that GOs accelerated PLLA crystallization from melt by increasing the nucleation density and addition of 0.1 wt% GO resulted in a small increase of equilibrium melting point but more GOs was unfavorable for the crystallites perfection of PLLA and resulted in a slight decrease of equilibrium melting point.

Xu ^[10] reported that GNSs could serve as heterogeneous nucleation agents of PLLA as well as CNTs, shortening the induction period of crystallization and accelerating the crystallization kinetics of PLLA, but the induction ability of GNSs was weaker

than that of CNTs. Additionally, more CNTs in PLLA from 0.05 to 0.1 wt % resulted in shortened induction period and enhanced crystallization rate, but the same increasing content of GNSs resulted in longer induction period and decreased crystallization rate. The crystallization mechanism of PLLA influenced by GNSs and CNTs was also discussed in detail. Xu ^[10] explained that in case of neat PLLA, the conformational ordering during crystallization begins with $-\text{CH}_3$ interchain interactions which preceded $-(\text{COtCH}_3)$ interchain interactions. Conversely, in the CNTs and GNSs nanocomposites, strong noncovalent binding between nanoparticles and PLLA main chains made the conformational ordering begin with $-(\text{COtCH}_3)$ interchain interactions which preceded $-\text{CH}_3$ interchain interactions, resulting in a direct reduce of induction period. This type of interchain interactions could be explained in terms of surface-induced conformational order (SICO). Furthermore, Xu ^[10] proposed that PLLA chains might prefer to align along CNTs axis and strict lattice matching between PLLA chains and the external graphitic sheet of CNTs is not required; whereas lattice matching play the dominant role in surface-induced crystallization of PLLA chains on GNSs surface, which made PLLA chains need more time to adjust their conformations, and PLLA single crystals on GNSs surface could show multiple orientations, which might impinge on adjacent single crystals and suppress the crystal growth.

The effect of coexistence of processing conditions and blending with other materials or additives on crystalline structures and crystallization behaviors of PLLA were also investigated as well as other polymers ^[23, 25, 27, 29-31, and 35]. Zhang ^[7] prepared highly oriented and amorphous PLLA/poly(D-lactide) (PDLA) with 1:1 blend of high-molecular-weight PLLA and middle-molecular-weight PDLA. After suitable annealing treatment, the obtained blend crystallized as α' form crystal together with stereocomplex β_c co-existing in the materials. Such results indicated that strong enough stretch of PLLA chains favors α' form crystal formation more than that of α form, which is different from the results of Huang *et al.* ^[5]. Perhaps, too strong stretch of PLLA chains inhibited the perfect adjustment of helical chain conformation and the ordered chain packing, resulting in disordered crystal as α' form instead of ordered α form. In the following heating process above 120 °C, the heavily stretched PLLA chains could relax to some extent and this α' form crystal could reorganize as oriented α form which melted around 180 °C. Further heating resulted in crystallization of molten chains on the surface of β_c crystallites with high degree of chain orientation revealing that β_c crystallites surface has model effects and could induce PLLA

molten chains to crystallize on it.

Among the mentioned additives, two-dimensional GNSs have emerged as a subject of enormous scientific interest due to its exceptional electron transport, mechanical properties, and high surface area [2, 10, 11, and 20-24]. The nucleation effect of GNSs and its influence on crystal structure and crystallization mechanism of PLLA have been investigated as well as the influences of other modification methods of PLLA. However, some details of the influence of GNSs on crystallization behaviors and crystalline structures of PLLA in PLLA/GNSs composite are not fully investigated. For example, the influence of GNSs on the spherulite growth rate and α' - α crystal formation transition of PLLA has been rarely reported. The crystallization mechanism of PLLA and the influences of GNSs on it need further explorations.

To understand the crystallization behaviors and crystallization mechanism of polymers, a crystallization theory of Hoffmann-Lauritzen with the popular expression given by Equation (1) has been developed and widely used to describe the temperature dependence of the growth rate u near the melting temperature [12]. Within such a temperature range, the growth rates are considered to be controlled by an activation step. As shown in Equation (1), the first exponential factor accounts for the temperature-dependent segmental mobility as given by Vogel-Fulcher equation with T_A and T_V referring to the activation temperature and Vogel temperature, respectively [51, 52]. The second exponential factor states that the height of the activation barrier diverges at T_f^∞ . That is, in Hoffmann-Lauritzen theory, the growth rate of polymer crystallites is usually taken for granted to be controlled by the supercooling below the equilibrium melting point of a macroscopic sample, T_f^∞ .

$$u = u_0 \exp\left(\frac{-T_A}{T - T_V}\right) \exp\left(\frac{-T_G}{T_f^\infty - T}\right) \quad (1)$$

Strobl [51] suspected that the activation energy does not diverge at T_f^∞ but much earlier at T_{zg} . He defined T_{zg} as the zero growth temperature which is another characteristic temperature for a system different from T_f^∞ . And T_{zg} can be identified with the temperature of the hidden transition between the melt and mesophase according to Strobl crystallization theory of polymers. Strobl [52] replaced T_f^∞ in Equation (1) with T_{zg} and Equation (2) was obtained. Then he reordered Equation (2) as Equation (3) with a differentiation of $\ln(u)$ with regard to T . By plotting $[-\ln(u/u_0)/dT + T_A/(T - T_V)^2]^{-1/2} \sim T$, T_{zg} of some polymers can be easily obtained according to the linear relation in Equation (3). For example, T_{zg} of poly(ϵ -caprolactone) (PCL) had been determined as 77 °C [51, 52], about 22 °C lower

than T_f^∞ of PCL. T_{zg} s of iPS and linear PE had been obtained as 275 °C and 132.5 °C, respectively. The existence of T_{zg} of the polymers supported the view of Strobl^[52], showing that the crystal growth is mediated by a transient mesophase with T_{zg} as the transition temperature between it and the melt.

$$u = u_0 \exp\left(\frac{-T_A}{T - T_V}\right) \exp\left(\frac{-T_G}{T_{zg} - T}\right) \quad (2)$$

$$\left(-\frac{d\ln(u/u_0)}{dT} + \frac{T_A}{(T - T_V)^2}\right)^{-1/2} = T_G^{-1/2}(T_{zg} - T) \quad (3)$$

In this paper, GNSs is added into PLLA by solution blending method. The crystal structures, crystallization morphology, crystallization behaviors including the nucleation process and spherulite growth of PLLA in the obtained PLLA/GNSs composite were investigated as well as those of pure PLLA by XRD, POM, SAXS, and DSC. The influences of GNSs on the crystal forms in PLLA/GNSs and pure PLLA isothermally crystallized at different crystallization temperatures T_c s were first examined to understand the influence of GNSs on the known α' - α crystal formation transition of PLLA. Then T_c s were selected to reveal the nucleation effect of GNSs and the influence of GNSs on the spherulite growth of α form PLLA during isothermal crystallization process. The resulting crystallization behaviors of PLLA in both PLLA/GNSs and pure PLLA were analyzed according to Strobl crystallization theory with the zero growth temperature T_{zg} s of α form PLLA in both PLLA/GNSs and pure PLLA determined. With further synchrotron on-line SAXS and DSC results of the variations of long period L of α form PLLA during isothermal crystallization process and the melting behaviors of both PLLA/GNSs and pure PLLA at different T_c s, the crystallization mechanisms of PLLA and the influence of GNSs were discussed.

2. Experimental

Materials

Poly(L-lactide) (PLLA) was supplied by Zhejiang HISUN biomaterial Co. Ltd, China. The weight average molecular weight (M_w) and the number average molecular weight (M_n) are 109,000 and 88,200 g/mol respectively. The differential scanning calorimetry (DSC) determined melting point of the PLLA is 172 °C.

Graphene nanosheets (GNSs) were carboxyl graphene powder productions purchased from Nanjing XFNANO Materials Tech Co., Ltd, which were prepared by thermal exfoliation reduction and hydrogen reduction. The carboxyl content is about 5%. The diameter is about 500 nm. The thickness is about 0.8-1.2 nm. The single

layer ratio is 80% and the purity is 99.8%.

Preparation of PLLA/GNSs composite

PLLA was solution blended with GNSs. First, 1 g PLLA was solved in 20 mL chloroform. Second, 1 mg GNSs was well dispersed and suspended in DMF by 20 min heating and stirring followed by 20 min ultrasonic treatment. Then the above PLLA solution and GNSs suspension were mixed together. With a slow enough addition of alcohol while stirring, PLLA and GNSs were precipitated together. The obtained flocculent precipitate was collected and dried in a vacuum chamber for 24 hours at 70 °C to remove the solvents.

Sample preparation and Characterization

A Linkam CSS450 shear stage (Linkam Scientific Instruments, Ltd., Tadworth, Surrey, U.K.) was used to prepare samples of pure PLLA and the prepared PLLA/GNSs composite at different isothermal crystallization temperatures for XRD, SAXS, and DSC measurement. The mechanical design and electronics of the Linkam shear stage provided a precise control of the needed temperature and sample thickness. An Olympus BX51 was used to obtain POM images. All samples were firstly melted at 200 °C for 1 min on the shear stage, which is connected with a heating and temperature control equipment. Then the upper lid was put on the melted samples, and then most of the bubbles were degassed. Then screw down the nuts on the upper lid, part bubbles were degassed during the process. Then screw up the nuts, screw down the nuts, after three times, bubbles could be avoided or mostly degassed. After the thermal history of the samples was erased, the samples were cooled with a cooling rate of 30 °C/min to pre-set temperatures for isothermal crystallization, which were selected as 86 °C, 96 °C, 106 °C, 116 °C, 126 °C, and 136 °C. After held at the pre-set isothermal crystallization temperatures enough time to crystallize, the samples were quickly cooled to 30 °C and carefully removed for investigation by ex situ XRD and DSC or in-situ SAXS.

XRD measurements were performed at room temperature using Rigaku D/max 2500V with a Cu-K α source ($\lambda = 1.54\text{\AA}$). The scanning speed is 2 °/min within the range of 10-35°. The voltage is 40 kV and the current is 200 mA.

The synchrotron SAXS measurements were carried out at beamline 1W2A ($\lambda = 1.54\text{\AA}$) of Beijing Synchrotron Radiation Facility (BSRF), Beijing, China. 2D-SAXS patterns were integrated to obtain 1D-SAXS profiles as a function of scattering vector. The detector Mar165CCD, with 2048×2048 pixels and the size of a pixel is 79.1 μm , is 1620 mm away from the sample. The long period of PLLA was

calculated according to one-dimension electron density correlation function as shown in reference ^[53].

DSC experiments were carried out using a Perkin-Elmer DSC-7, the heating rate was 10 °C /min. The samples of about 10 mg were protected by N₂. The experimental temperature range was selected from room temperature to 200 °C.

3. Results and Discussions

3.1. Crystal structures

Since different crystals can be formed in PLLA and the formed crystal structures are dependent on the crystallization temperatures T_c s ^[12], the influence of GNSs on the crystals formation of PLLA in PLLA/GNSs composite at different T_c s were first examined. Fig. 1 (a1) shows the XRD profiles of pure PLLA isothermally crystallized at various T_c s from melt. Fig. 1 (a2) and (a3) provide partially enlarged XRD profiles of those in Fig. 1 (a1) for pure PLLA. In these XRD profiles of pure PLLA, the most intense peaks can be observed at $2\theta=16.54^\circ$ for T_c s above 116 °C, which agrees well with the most intense peaks in the WAXS profiles of PLLA locating at $2\theta=16.70^\circ$ for T_c s above 120 °C reported by Kawai *et al.* ^[12]. The peak at $2\theta=16.54^\circ$ can be attributed to (110) and/or (200) planes. Another strong reflections of (203) and/or (113) planes can also be observed for T_c s above 116 °C. And both these two strong peaks remained when T_c 's smaller than 116 °C; whereas several reflections such (010) and (210) are relatively weak. Since it is known that only α form PLLA can form when T_c is higher than 120 °C, the XRD profiles in Fig. 1 (a1) - (a3) for T_c s above 116 °C can be assigned to be orthorhombic α form PLLA, in which the PLLA molecules are assumed to have a left-handed 10₃ helical conformation ^[12, 54].

For T_c s below 116 °C, the intensity of some diffraction peaks, including (103)/(004), (1010), and (010), which are characteristics of α form crystal, decreased with decreasing T_c , and finally disappeared at $T_c=86$ °C. At the same time, some diffraction peaks, including (200)/(110) and (203)/(113), shifted to smaller 2θ values, which were further shown in Fig. 2 (a) and (b). These changes of the peaks in XRD profiles of PLLA indicated that α form content decreased while α' form content increased within the isothermally crystallized samples with decreasing T_c till only α' form formed below $T_c=86$ °C. This agrees with the results of many researchers who regarded the disappearance of the (010) reflection as the indications of crystal formation transitions from co-existence of both α and α' form to only α' form PLLA ^[3, 5, 55].

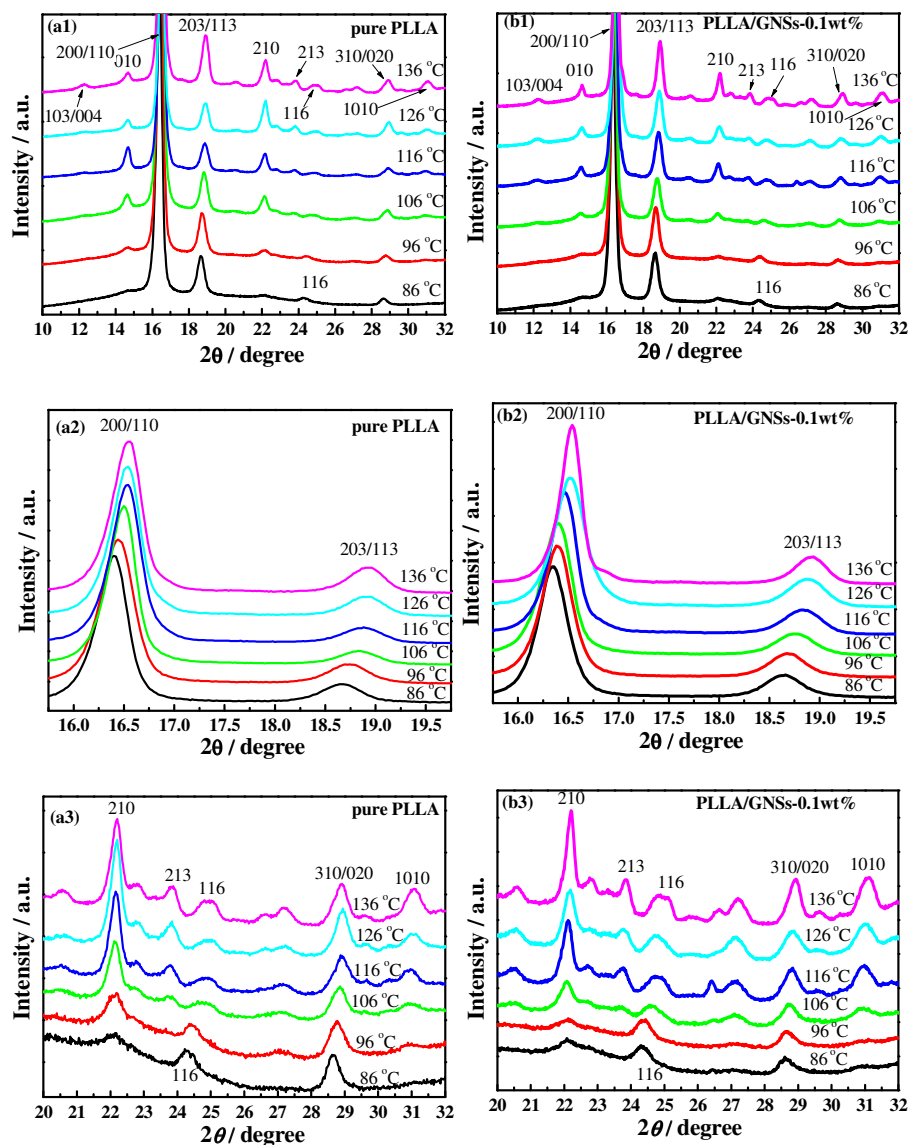


Fig. 1 XRD profiles of pure PLLA and PLLA/GNSs composite samples isothermally crystallized at various T_c s from melt (a1)-(a3) pure PLLA; (b1)- (b3) PLLA/GNSs-0.1wt% composite

Kawai *et al.* [12] have proved that the disappeared diffraction peaks of (103)/(004), (1010), and (010) in Fig. 1 (a1) - (a3) were not due to the crystallinity decrease with decreasing T_c , but due to the crystal structure for lower T_c s which is different from the α form PLLA at higher T_c s. And it seems to be secure to assume this different crystal structure as α' form PLLA [1, 5-7, and 12-16], which has a hexagonal packing since the absence of some diffractions can be well explained by the extinction rule of the hexagonal lattice. This was supported by the conclusion drawn from IR measurements by Zhang *et al.* [15, 56], which revealed that the PLLA chain has the same 10_3 helical

conformation for all T_c s when it is crystallized from the melt and precluded the possibility of β phase formation at low T_c s, proposed by Kawaguchi *et al.* [57]

In Fig. 2 (a) and (b), within the experimental range of T_c s, three regions can be observed for pure PLLA sample: (i) α' form PLLA below $T_c \approx 86^\circ\text{C}$; (ii) $\alpha' \leftrightarrow \alpha$ crystal formation transition with $86^\circ\text{C} < T_c < 116^\circ\text{C}$; (iii) α form PLLA above $T_c \approx 116^\circ\text{C}$. These three regions agree with the results of Kawai *et al.* [12], who concluded by both WAXS and SAXS that the “pure” α' form might be a limit disordered crystal with hexagonal packing of the 10_3 helix of the PLLA chain and this “pure” α' form can only be obtained when T_c is below 90°C . This is somewhat different from the results of Zhang *et al.* [15], who revealed that the α' form is obtained below 120°C .

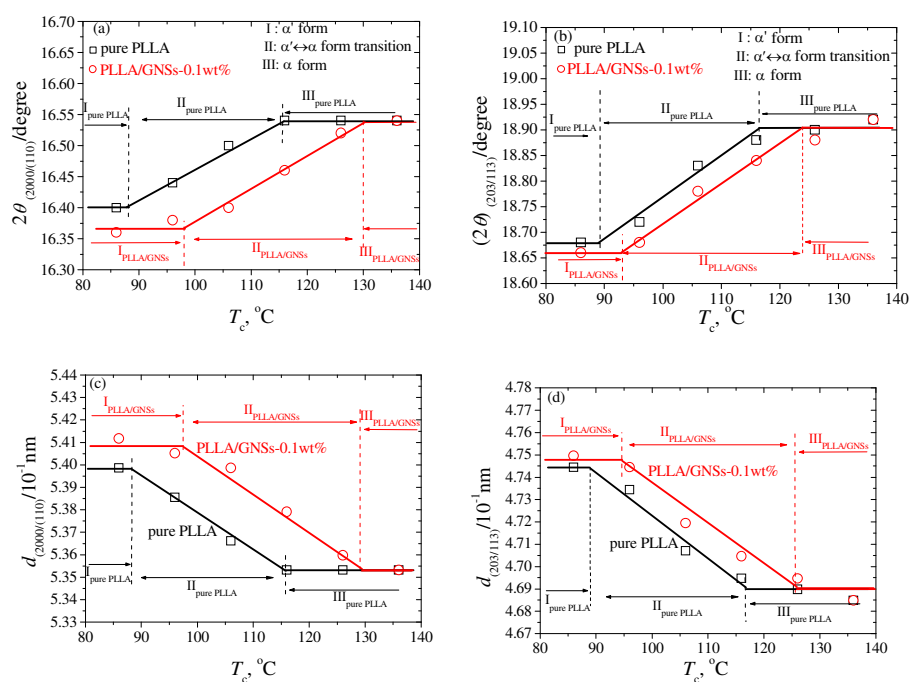


Fig. 2 2θ values from (200)/(110) and (203) diffractions (a and b) and the corresponding d values calculated from Bragg Equation (c and d) of PLLA and PLLA/GNSs composite samples crystallized at various T_c 's from the melt. The lines are plotted to guide eyes

Actually, it is difficult to differentiate the crystal structures of pure PLLA samples only from their XRD profiles shown in Fig. 1 (a1), because the crystal structure of α' form PLLA is quite similar to that of α form, except for the chain conformation and chain packing mode [5, 58]. Since it has been known that there are only α' crystal and α crystal formed in the PLLA samples isothermally crystallized at 86°C and 126°C , respectively. It is reasonable to regard the (203) reflection peak as one single sharp reflection in XRD profiles of the samples with T_c s of 86°C and 126°C . For PLLA

samples crystallized at T_c s higher than 86 °C and lower than 126 °C, the (203) reflections can be resolved into two components originating from the co-existing α' and α forms PLLA. From this point of view, the observed three regions and their relations to crystal forms of PLLA in Fig. 2 (a) and (b) within the experimental range of T_c s are acceptable.

Fig. 1 (b1) shows the XRD profiles of PLLA/GNSs-0.1wt% composite isothermally crystallized at various T_c s from melt. In Fig. 1 (b2) and (b3), these XRD profiles were partially enlarged to show the variations clearly. While one compared those XRD profiles of the composite with those of pure PLLA in Fig 1 (a1)-(a3), one could find that 2θ values of some diffraction peaks, such as (200)/(110), (203)/(113), and so on, of PLLA/GNSs composite sample also shifted to smaller values with decreasing T_c s, shown in Fig. 2 (a) and (b). This proved that the α' form at low T_c s, α' - α crystal formation transition, and α form at high T_c s of PLLA also appeared in PLLA/GNSs composite. Interestingly, it was found that the 2θ - T_c curves of PLLA/GNSs composite sample seemed to have been moved to higher T_c and smaller 2θ comparing with those curves of pure PLLA within the region of α' - α crystal formation transition.

At high enough T_c , the 2θ values of (200)/(110) and (203)/(113) peaks of XRD profiles of both PLLA/GNSs composite and pure PLLA samples tended to be equal. According to the corresponding d values calculated from Bragg Equation of pure PLLA and PLLA/GNSs composite samples crystallized from the melt at various T_c s and shown in Fig. 2 (c) and (d), the α form PLLA in both the two samples have the same crystalline structure at high enough T_c s. That meant that the crystalline structure of α form PLLA was not affected by the added GNSs. With decreasing T_c , PLLA/GNSs composite enter into the α' - α crystal formation transition region earlier than pure PLLA sample and its d values much larger than those of pure PLLA sample at the same T_c s. With T_c decreasing further, PLLA/GNSs composite left α' - α crystal formation transition region and enter α' form region, while the d values of α' form PLLA in PLLA/GNSs composite is obviously much larger than those in pure PLLA sample. The structure of α' form PLLA was influenced by GNSs addition and tended to be more unstable at T_c s below the α' - α crystal formation transition, which is different from what happened for stable α form PLLA without any variations of d values at high T_c s above the α' - α crystal formation transition.

Additionally, in Fig. 2, it is revealed that the added GNSs apparently promoted the crystal formation transition from α form PLLA to α' form PLLA within the T_c ranges

for co-existence of both the two crystals; as if α' form PLLA was preferred more than α form PLLA. That is, GNSs were especially helpful for PLLA to form less stable α' crystal instead of more stable α crystal. If more α' crystal were formed in a sample, there would leave less PLLA molecular chains to form α crystal. There was competition between the formation of α' crystal and that of α crystal in the samples. This made the primitive α' - α crystal formation transition region in pure PLLA shifted to higher temperatures once GNSs were distributed into this material. GNSs made it much easier for α' crystal to appear even at T_c s higher than 120 °C, under which it was reported that only α crystal can form in pure PLLA. It is indicated that the GNSs slices could encourage the PLLA chains to enter the crystal quickly and they seemed to have no enough time to be well organized to form stable and perfect α crystals, even have no enough time to form less stable but dense α' crystal in the PLLA/GNSs composite as in pure PLLA.

From Fig. 1 and Fig. 2, it can be concluded that high enough T_c s is in favor of perfect crystalline structure formation of α form PLLA and low enough T_c makes for only α' form PLLA in both pure PLLA and PLLA/GNSs composite samples. The crystalline structure of α form PLLA at T_c s above the α' - α crystal formation transition was not affected by GNSs, which agreed with Wang *et al.*^[50] who reported that both PLLA and PLLA/GOs had the same crystal structure at 130 °C; whereas, the non-perfect α' form PLLA was influenced and tended to be less perfect at T_c s below the α' - α crystal formation transition. At the same time, GNSs existence in PLLA favors α' crystal formation more than α crystal formation and the α' - α crystal formation transition was shifted to higher temperatures. Such effects of GNSs were different from those of melt shear^[5], PDLLA^[6] and DBS^[8] which all favor α crystal formation more inversely and result in shifts of α' - α crystal formation transition towards low temperatures. And melt shear was found to accelerate nucleation of PLLA^[5], while PDLLA and DBS could decrease crystallization rate of PLLA^[6, 8]. To understand the influence of GNSs on crystal structures of PLLA further, the crystallization behaviors of PLLA in the composite should be examined and PLLA crystallization mechanism need to be discussed.

3.2. Crystallization behaviors

In order to know whether the crystallization behavior of PLLA/GNSs-0.1wt% composite is different from that of pure PLLA or not, the POM images of both the two materials isothermally crystallized at different T_c s above α' - α crystal formation transition during their isothermal crystallization process were obtained. Thus, the

effects of GNSs on the crystallization behavior of α form PLLA were examined.

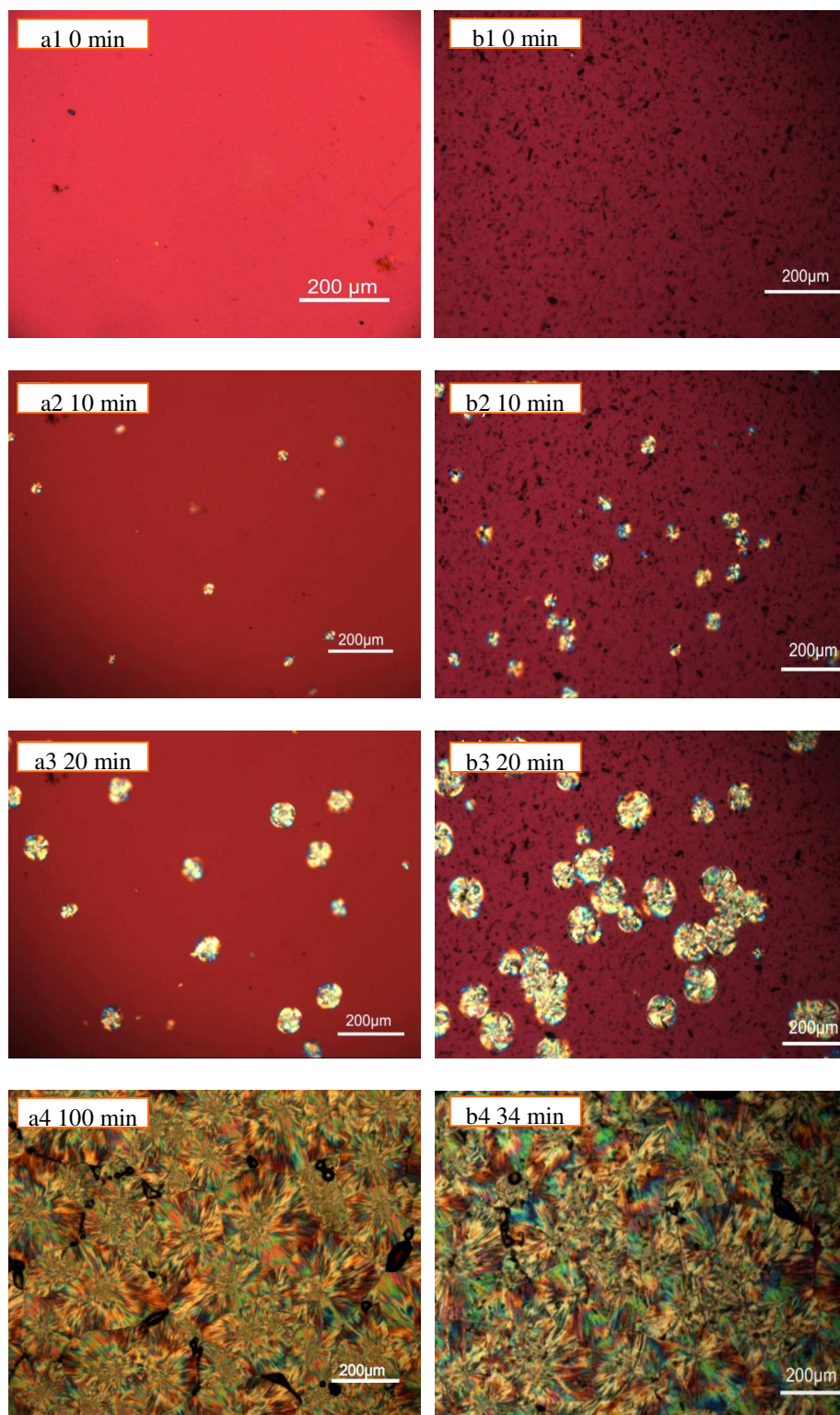


Fig. 3 POM images of PLLA and PLLA/Graphene composite samples isothermally crystallized at $T_c = 140^\circ\text{C}$ from melt during their isothermal crystallization process. (a1)-(a4) pure PLLA, (b1)-(b4) PLLA/GNSs -0.1wt% composite

Fig. 3 shows the typical POM images of the samples at $T_c = 140$ °C. From Fig. 3, it can be seen that PLLA spherulites were well formed both in pure PLLA and PLLA/GNSs-0.1wt% composite samples during their isothermal crystallization process. This implied that PLLA spherulites formation was not disturbed by GNSs in PLLA/GNSs-0.1wt% composite. While comparing the POM images in Fig. 3 (a1)-(a3) with those in Fig. 3 (b1)-(b3), one can observe more PLLA spherulites formed in PLLA/GNSs-0.1wt% composite than in pure PLLA at the same isothermal crystallization time with $T_c = 140$ °C within the first 20 min of the crystallization process. This revealed that the nucleation density of α form PLLA in PLLA/GNSs-0.1wt% composite is much higher than that of the pure PLLA sample. That is, the addition of GNSs into PLLA accelerated the nucleation process of PLLA.

From Fig. 3 (a4) and (b4), it can be noticed that 100 min and 34 min were needed for PLLA spherulites in pure PLLA and PLLA/GNSs-0.1wt% composite samples, respectively, to grow full of the observed range of the POM images. The obtained PLLA spherulites in pure PLLA seemed to be slightly larger than those in PLLA/GNSs-0.1wt% composite sample, which confirmed the higher nucleation density of PLLA in the composite as revealed in Fig. 3 (a1)-(a3) and (b1)-(b3). This proved that GNSs could serve as nucleating agents in accelerating the crystallization kinetics of PLLA, agreeing with Xu^[10].

In fact, not only the increased nucleation density of PLLA spherulites in PLLA/GNSs-0.1wt% contributed to the higher crystallization rate of PLLA in the composite than that in pure PLLA. The enlarged PLLA spherulite growth rate due to addition of GNSs also played important roles. To understand this, the diameters of PLLA spherulites depending on isothermal crystallization time during crystallization process were obtained and shown in Fig. 4 for both pure PLLA and PLLA/GNSs-0.1wt% composite samples. From the slopes of the fitted lines in Fig. 4, the radius growth rates of the PLLA spherulites were determined and shown in Fig. 5.

According to the crystallization theory, the crystal growth rate always shows well-known bell-shaped temperature dependence. This is also found to be true for pure PLLA and PLLA/GNSs-0.1wt% composite samples. It can be found in Fig. 5 that the radius growth rate of PLLA spherulite of pure PLLA reached its peak value at about $T_c = 130$ °C. This experimental result agrees very well with those reported by Kawai and his coworkers^[12]. Importantly, at all the experimental crystallization temperatures, the radius growth rates of PLLA spherulite of PLLA/GNSs-0.1wt% composite sample were found larger than those of pure PLLA sample. GNSs can

accelerate the radius growth of PLLA spherulite, but it does not change the well-known bell-shaped temperature dependence of the radius growth rate. GNSs in PLLA/GNSs-0.1wt% composite even had no influence on the position of the peak growth rate at about $T_c = 130$ °C. From this point of view, the faster crystallization process of PLLA in PLLA/GNSs-0.1wt% composite than that of pure PLLA can be attributed to the combination of the faster nucleation process and the faster radius growth of the spherulite of PLLA in PLLA/GNSs-0.1wt% composite than that in pure PLLA.

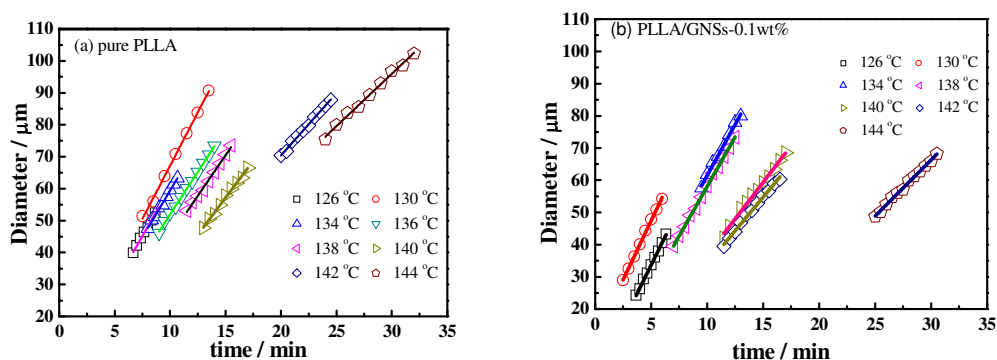


Fig. 4 Diameter growth of spherulites of PLLA and PLLA/GNSs composite samples isothermally crystallized at various T_c s from melts. (a) pure PLLA, (b) PLLA/GNSs-0.1wt%

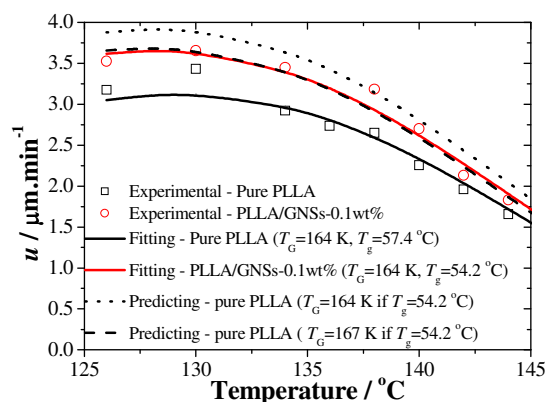


Fig. 5 Radius growth rates u of the spherulites of PLLA in pure PLLA and PLLA/GNSs composite samples as functions of crystallization temperature (T_c). Solid lines are obtained by fitting the experimental data according to Equation (3) with $T_{zg} = 177$ °C and $T_G = 164$ K. The dotted and dashed lines are the predicting results of pure PLLA according to Equation (3) with $T_{zg} = 177$ °C and T_G of 164 K and 167 K, respectively, if T_g is set equal to that of PLLA/GNSs of 54.2 °C

The DSC curves of pure PLLA and PLLA/GNSs-0.1wt% composite samples during non-isothermal crystallization process with a temperature decreasing rate of 10 °C /min from melts shown in Fig. 6 supported the above POM observations. With

temperature decreasing, the DSC curve of pure PLLA sample showed one exothermic peak. Similarly, PLLA/GNSs-0.1wt% composite also showed one exothermic peak. However, its thermal enthalpy is much larger and the corresponding temperature of the crystallization peak is higher than those of the pure PLLA sample. The thermal enthalpy difference of the two samples implied that GNSs in PLLA/GNSs-0.1wt% composite resulted in higher crystallinity of its PLLA matrix. In pure PLLA sample, with temperature decreasing, low nucleation rate and slow radius growth rate of the spherulite apparently left no enough time for the concerned PLLA molecular chains to form crystalline. When GNSs added, both the nucleation rate and the radius growth rate of the spherulite are increased. Thus, the total crystallization rate of PLLA is enhanced by GNSs comprehensively in the composite.

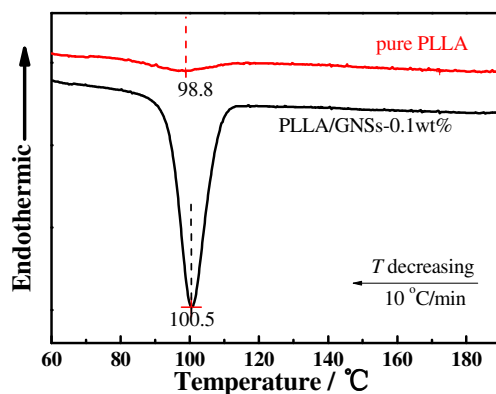


Fig. 6 DSC curves of Non-isothermal crystallization process of PLLA in pure PLLA and PLLA/GNSs composite samples with a temperature decreasing rate of 10 °C/min from melts

It seemed that the added GNSs can provide more chances for more PLLA molecular chains to form crystalline structure within the limited time range before they are cooled to lose enough mobility due to decreasing temperature. It is really an interesting observation. Since GNSs in the composite may act as “physical walls” interacting with the PLLA molecular chains, theoretically the number of chain configurations should decrease and hence there is less mobility of the PLLA chains which would leave less chance of crystallites to form. However, the opposite was observed here. Maybe the sum of attraction forces along a chain is lower in the presence of a physical wall like a GNS. This leads to less configurational possibilities of PLLA chains – however also to a much higher mobility hence favoring crystallinity.

To find out the effects of GNSs addition on the mobility of PLLA molecular chains in PLLA/GNSs composite, further DSC measurements were executed to determine

the glass transition temperatures of PLLA in pure PLLA and in the composite. The isothermally crystallized samples at different crystallization temperatures T_c were adopted and the onset temperatures of the glass transition were obtained. The T_c s were selected as 86, 96, 106 and 116 °C and the results were shown in Fig. 7 as examples. The glass transition temperature $T_{g,onset}$ of PLLA in pure PLLA was determined as about 57.4 °C and it was found almost independent on T_c . Importantly, the $T_{g,onset}$ of PLLA in PLLA/GNSs composite was about 54.2 °C, also independent on T_c , and it was really found lower than $T_{g,onset}$ of pure PLLA. This meant the added GNSs in the composite increased the mobility of PLLA molecular chains.

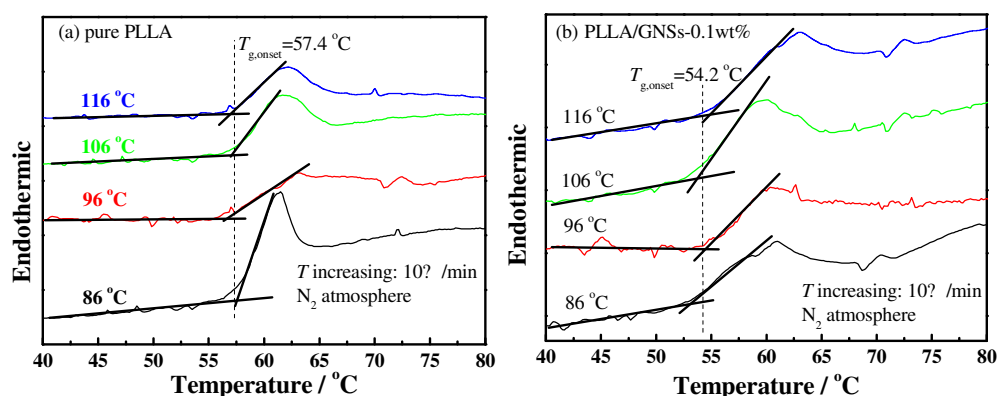


Fig. 7 Determination of glass transition temperatures of PLLA by DSC with a temperature increasing rate of 10 °C/min for the samples isothermally crystallized at different T_c s. (a) pure PLLA, (b) PLLA/GNSs-0.1wt%

As known, in PLLA main chains, there are many structures of $-(COCH_2CH_2O)_n-$ resulting in strong interchain interactions by hydrogen bonds, while on the surface of GNSs slices there are no such polar functional groups. This decrease of $T_{g,onset}$ of PLLA due to the existence of GNSs in PLLA may be possible. Perhaps the interactions between PLLA chains were weakened since the interactions between GNSs and PLLA chains may be much weaker. The dispersed GNSs in PLLA resulted in replacement of relatively strong interactions between PLLA chains by somewhat weaker GNSs-PLLA chain interactions. This could be supported by Patti^[59] who proved by molecular dynamics simulations that small nanoparticles can act as plasticizers in polymeric matrix. Xiao *et al.*^[60] reported that the plasticized poly(lactic acid) with triphenyl phosphate (TPP) could increase the spherulite growth rate. Of course, for PLLA chains with too low mobility to form crystallization nucleus, increased chain mobility would help PLLA chains to enhance the nucleation density. This well interpreted why GNSs can accelerate crystallization process of PLLA.

The kinetic data in Fig. 5 can be reorganized and linearly fitted by plotting $[-\ln(u/u_0)/dT+T_A^*/(T-T_V)^2]^{-1/2} \sim T$ according to Equation (3) and the results were shown in Fig. 8. Here, $T_A=754$ K was obtained from $T_A=U^*/R$ with $U^*=1500$ cal/mol and $T_V=T_g-30$ K was selected according to reference [12]. With the linear fitting parameters of $T_{zg}=177$ °C and $T_G=164$ K for both pure PLLA and PLLA/GNSs in Fig. 8, the fitted curves of growth rate u dependent on T_c were calculated and shown back in Fig. 5 to compare with those experimental data. The results showed that both the growth rates of pure PLLA and PLLA/GNSs could be fitted well. Thus, the zero growth temperature T_{zg} of PLLA was determined as 177 °C and it was found there was no observable influence of the added GNSs on it.

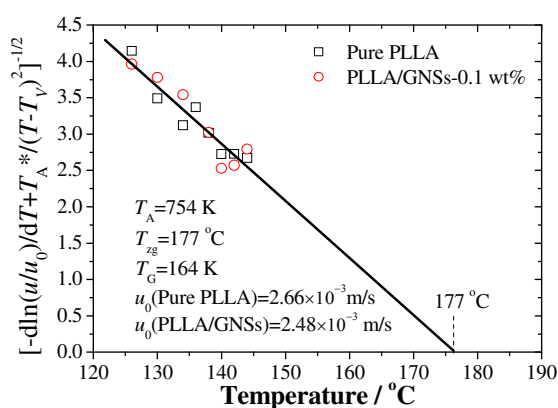


Fig. 8 Analysis of PLLA spherulite growth rate data of pure PLLA and PLLA/GNSs-0.1 wt% composite by fitting with Equation (3) according to Strobl crystallization theory

As for pure PLLA, the $T_{zg}=177$ °C of α crystal is found smaller than its $T_f^\infty=192.8$ °C reported by Yeh [55] for their PLA 4032D with a melting point of 168 °C. Tsuji [61] reported even higher T_f^∞ for their samples, in the range from 198 to 212 °C and Kawai *et al.* [2] gave $T_f^\infty=215$ °C. Since the used PLLA here has a melting point of 172 °C higher than 168 °C, the T_f^∞ may be higher than 192.8 °C. This implies pure PLLA may have a T_{zg} lower than its T_f^∞ . Importantly, the T_{zg} and T_G values of α form PLLA in PLLA/GNSs are found equal to those of α crystal in pure PLLA, only with the u_0 values slightly different.

According to Equation (2), lower T_g of PLLA favors larger growth rate u . But according to Equation (3), at temperature near T_{zg} , growth rate u tends to be very small and the T_g variation of PLLA will have little influence on T_{zg} of α form PLLA. This indicated that the GNSs-induced increase of PLLA segmental mobility does not affect the T_{zg} value and only results in decrease of T_G , which has been supported by the fitting results according to Equation (3) in Fig. 8. With increasing T_c , the decrease

of spherulite growth rate of PLLA in PLLA/GNSs was accompanied by a synchronous reduce of the acceleration effects of GNSs on growth rate. It seemed that GNSs had no impact on the thermodynamic essence of the investigated isothermal crystallization process of PLLA, though it can help PLLA spherulites kinetically grow faster. Or the influence of GNSs on the isothermal crystallization thermodynamics is too weak to be observed. This may be helpful to understand the effects of GNSs on the crystallization process and the crystallization mechanism of PLLA.

Supposing that T_g of pure PLLA decreased from 57.4 °C to 54.2 °C equal to that of PLLA in PLLA/GNSs, a predicting line shown as the dotted line in Fig. 5 could be obtained if the fitting parameters $T_{zg}=177$ °C, $T_G=164$ K, and $u_0=2.66\times 10^{-3}$ m/s obtained in Fig. 8 were used. It can be seen that the values of the growth rate u at different T_c s are obviously larger than the experimental data and the fitting line of PLLA/GNSs according to Strobl crystallization theory. When the value of T_G was adjusted to 167 K, the predicting dashed line for pure PLLA in Fig. 5 could overlap well together with the fitting line of PLLA/GNSs. This implied that the increase of growth rate u of PLLA in PLLA/GNSs, when comparing with that of PLLA in pure PLLA, is mainly due to the increase of segmental mobility of PLLA chains because of addition of GNSs. At the same time, the contribution of the increased segmental mobility seemed to have been inhibited by GNSs which have certain steric hindrance to spherulite growth. This agrees with the results of Xu^[10] who find 0.05 wt% content of GNSs in PLLA could serve as heterogeneous nucleation agents of PLLA, shortening the induction period of crystallization and accelerating the crystallization kinetics of PLLA. However, if GNSs content increased to 0.1 wt%, it resulted in longer induction period and decreased crystallization rate of PLLA, because PLLA single crystals on GNSs surface may suppress the crystal growth.

3.3. Lamellar parameter

To further understand the influence of GNSs on the crystalline structure of PLLA, pure PLLA and PLLA/GNSs composite samples were both isothermally crystallized at 145 °C to form α form PLLA and the 2D SAXS patterns of them were collected. Some typical patterns were selected and shown in Fig. 9. Corresponding to the 2D SAXS patterns, 1D SAXS intensity profiles were plotted and shown in Fig. 10.

From Fig. 9 (a1) and (b1), no observable scattering circles related to crystalline structures of PLLA can be found, indicating that all the crystalline structures in the two samples had already been removed when melted. In Fig. 10 (a) and (b), no crystalline peaks appeared in both the two samples. With crystallization time

increasing, one scattering circle appeared in the 2D SAXS patterns in Fig. 9 and crystalline peaks appeared in the 1D SAXS intensity profiles in Fig. 10. Then the intensity of the scattering circles of both the two samples increased with increasing crystallization time till the samples crystallized completely. From the variations of the intensity of the crystalline peaks in Fig. 10, the inducing crystallization time of pure PLLA and PLLA/GNSs composite samples were determined as 14 min and 7 min, respectively. And the two samples finished their crystallization processes at about 63 min and 45 min, respectively. This agrees with POM observations.

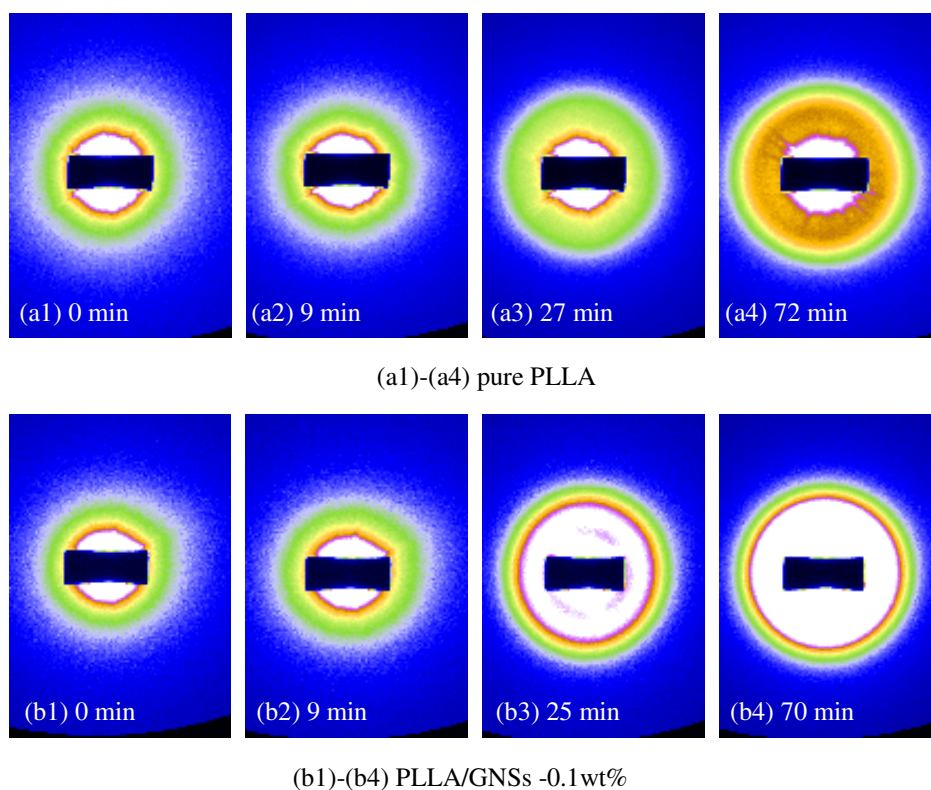


Fig. 9 2D SAXS patterns of pure PLLA and PLLA/GNSs composite samples isothermally crystallized at 145 °C (a1)-(a4) pure PLLA, (b1)-(b4) PLLA/GNSs -0.1wt%

Fig. 11 shows the long periods of PLLA in pure PLLA and PLLA/GNSs composite samples isothermally crystallized at 145 °C dependent on crystallization time. During the crystallization processes, long periods, L , of the two samples decreased with increasing isothermal crystallization time and finally reached constant values when crystallization processes finished. Those L values of PLLA/GNSs composite were found much smaller than those of pure PLLA and the revealed crystallization process finished much earlier than that of pure PLLA.

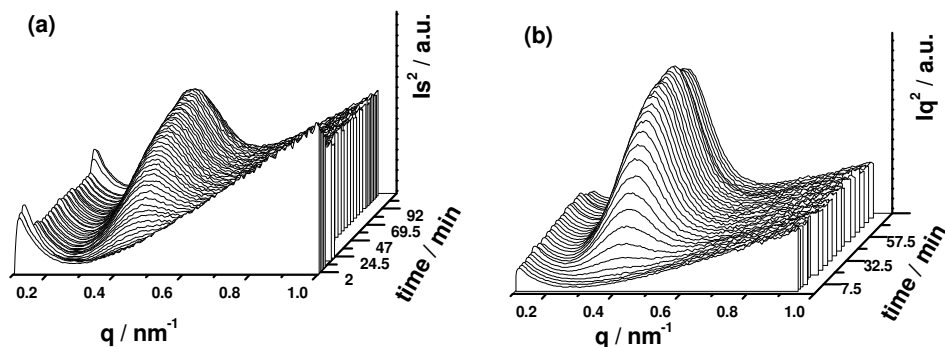


Fig. 10 1D SAXS intensity profiles of pure PLLA and PLLA/GNSs composite samples isothermally crystallized at 145 °C (a) pure PLLA, (b) PLLA/GNSs -0.1wt%

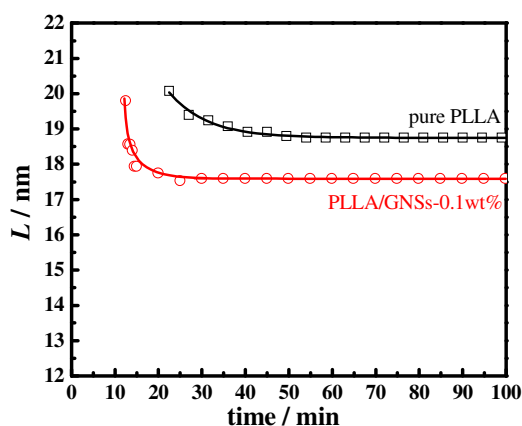


Fig. 11 Lamellar parameter L of PLLA in pure PLLA and PLLA/GNSs composite samples isothermally crystallized at 145 °C as a function of crystallization time

These phenomena can be interpreted successfully by Dual-lamellar stack model^[62]. At the initial stage of the isothermal crystallization process, some thick lamellar structures were formed first, and then some later formed lamellar structure inserted into the first formed ones, which resulted in decreasing long period, L , during isothermal crystallization process until the process finished. The phenomenon has also been found in other crystalline polymeric systems^[23, 27].

3.4. Melting behaviors

As known, melting behaviors are closely related to the crystallization behaviors and the resulted crystalline structures of crystalline or semi-crystalline polymers. Fig. 12 shows the melting behaviors of pure PLLA and PLLA/GNSs composite samples isothermally crystallized at various T_c s from melts revealed by DSC curves. According to the XRD profiles, only α form PLLA were formed at $T_c=136$ °C and only α' form PLLA were formed at $T_c=86$ °C in pure PLLA sample. At $T_c=106$ °C and

$T_c=96$ °C, within α' - α crystal formation transition region, both α and α' form PLLA were formed in pure PLLA sample. Because α form PLLA is more perfect than α' form PLLA, the melting point of α form PLLA is higher than that of α' form PLLA. The pure PLLA isothermally crystallized at $T_c=136$ °C showed a melting point of $T_m=173.0$ °C, which is higher than $T=170.5$ °C of the pure PLLA isothermally crystallized at $T_c=86$ °C. $T_m=173.0$ °C can be attributed to melting behavior of α form PLLA formed at $T_c=136$ °C, while $T=170.5$ °C can not be directly attributed to the melting behavior of α' form PLLA formed at $T_c=86$ °C. In fact, from the DSC curve of pure PLLA isothermally crystallized at $T_c=86$ °C, an exothermic peak at 152.2 °C can be found lower than the obvious endothermic melting peak at $T=170.5$ °C. This exothermic peak can be attributed to α' - α crystal transition while temperature increasing^[12]. So $T=170.5$ °C should be attributed to the melting behavior of those reformed α form PLLA in pure PLLA sample isothermally crystallized at $T_c=86$ °C. Interestingly, it seemed that all those α' form PLLA, formed at $T_c=86$ °C, melted and recrystallized as α form PLLA with increasing temperature from a temperature lower than 86 °C to a temperature higher than 180 °C, which makes it difficult to find the endothermic peak related to melting behavior of α' form PLLA isothermally crystallized at $T_c=86$ °C. Perhaps, the appearance of the exothermic peak at 152.2 °C revealed that the endothermic therapy of α' form PLLA was less than the exothermic therapy of α' - α crystal transition of PLLA in this pure PLLA sample isothermally crystallized at $T_c=86$ °C.

In the DSC curve of pure PLLA isothermally crystallized at $T_c=96$ °C, an exothermic peak at 156.2 °C appeared, which is higher than that exothermic peak at 152.2 °C of the sample isothermally crystallized at $T_c=86$ °C. And the endothermic peak of melting behavior of the reformed α form PLLA transited from α' form PLLA increased from $T_m=170.5$ °C of the sample isothermally crystallized at $T_c=86$ °C to $T_m=171.5$ °C of the sample isothermally crystallized at $T_c=96$ °C. This implied that the α' form PLLA in the sample isothermally crystallized at $T_c=96$ °C is more perfect than that in the sample isothermally crystallized at $T_c=86$ °C. More perfect α' form PLLA needs higher temperature to melt and transit into more perfect α form PLLA. With T_c increasing higher than $T_c=96$ °C within α' - α crystal formation transition region, less α' form PLLA in the sample results in smaller exothermic peak while melting, which may be smaller than the endothermic melting peak of these α' form PLLA. For example, as shown in Fig. 12 (a), the DSC curve of the sample isothermally crystallized at $T_c=106$ °C showed a small endothermic peak at $T=160.7$ °C, which is

resulted from the competition between α' - α crystal transition and melting process of α' form PLLA.

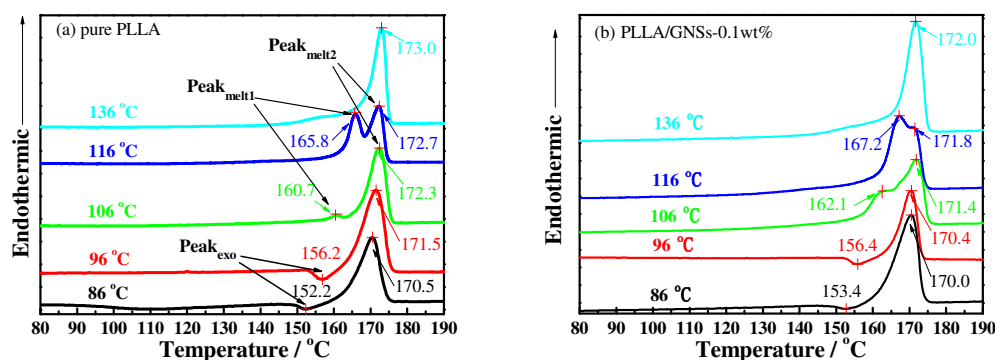


Fig. 12 DSC heating thermographs of pure PLLA and PLLA/GNSs composite samples isothermally crystallized at various T_c s from the melt (a) pure PLLA, (b) PLLA/GNSs -0.1wt%

When GNSs are added into PLLA, the melting behaviors of the composite samples isothermally crystallized at different T_c s, shown in Fig. 12 (b), are almost similar to those of the pure PLLA samples. The T_m s of the α form PLLA in PLLA/GNSs-0.1wt% sample formed during isothermal crystallization process or reformed from α' - α crystal transition process are lower than those of the α form PLLA in the pure PLLA sample at $T_c=96$ °C, 106 °C and 136 °C, respectively. This indicated that addition of GNSs into PLLA does not change the crystalline forms but prevents the molecular chains of PLLA from forming perfect crystalline structures, because GNSs accelerates the crystallization process and leaves no enough time for PLLA chains to adapt as completely as possible to the strict geometric space of perfect crystals.

Additionally, it can be found in Fig. 12 (a) and (b) that α' - α form transformation temperature and T_m s of α' form PLLA in PLLA/GNSs-0.1wt% sample are higher than those of the pure PLLA sample. Addition of GNSs into PLLA improved the perfectness of α' form PLLA. The influence of GNSs on the formation of α' form PLLA is different from that of α form PLLA.

3.5. Crystallization mechanism

As revealed in Fig. 5, the addition of GNSs does not change the temperature corresponding to the fastest radius growth rates u of the spherulites of PLLA. At about $T_c >130$ °C, the mobility of PLLA molecular chains in both the pure PLLA and PLLA/GNSs-0.1wt% samples are high enough to form a crystal. This meets with the

thermodynamic condition of formation of α form PLLA, whose formation is controlled by thermodynamic process^[4, 6, and 8]. Addition of GNSs into PLLA seems to have no influence on the thermodynamics of formation of α form PLLA. The larger radius growth rates u of the PLLA spherulites in PLLA/GNSs-0.1wt% than those in pure PLLA can mainly be attributed to the increase of the segmental mobility of PLLA chains due to addition of GNSs. The existing GNSs help PLLA molecular chains enter crystals faster. This is supported by the same zero growth temperature T_{zg} of PLLA in PLLA/GNSs to that of pure PLLA.

Perhaps, during crystallization process of PLLA, the segmental mobility of the PLLA molecular chains in PLLA/GNSs-0.1wt% is too fast to adapt perfectly into the crystals or the steric hindrance of GNSs to spherulite growth makes it difficult to form perfect crystals. Thus, the formed α form PLLA in PLLA/GNSs-0.1wt% sample is less perfect than that in pure PLLA sample, resulting in lower T_m of α form PLLA in PLLA/GNSs-0.1wt% sample than in pure PLLA sample which were isothermally crystallized at $T_c = 136$ °C. This was supported by the smaller long period L of α form PLLA in PLLA/GNSs than that in pure PLLA at 145 °C. Even in the α' - α crystal formation transition range, T_{ms} of α form PLLA in PLLA/GNSs-0.1wt% are lower than those in pure PLLA and both of the T_{ms} of α form PLLA in the two samples decreased with decreasing T_c . It seemed that the effect of GNSs is not obviously conflicted with the low molecular mobility at low temperatures. Perhaps, only those PLLA chains with strong enough mobility but without the steric hindrance of GNSs to spherulite growth can form perfect α form crystal.

Within the α' - α crystal formation transition range, introduction of GNSs resulted in α' form PLLA with more perfect crystal structures in PLLA/GNSs-0.1wt% than in pure PLLA at the same T_c . In this temperature range, the mobility of PLLA molecular chains in the pure PLLA sample is too low, resulting in less perfect crystals and low crystallization speed. The existence of GNSs can enhance the mobility of PLLA chains and help them enter α' form crystal in a more perfect way. So at the same time, GNSs can improve the perfectness of the formed crystals. These effects of GNSs on α' form PLLA formation are different from those effects on α form PLLA formation. The formation of α' form PLLA has been reported to be controlled by its kinetic mechanism^[4, 6, and 8] instead of its thermodynamic mechanism. The different effects of GNSs on α and α' form PLLA should be attributed to their different formation mechanism. With decreasing T_c in the α' - α crystal formation transition range, T_{ms} of α' form PLLA in both PLLA/GNSs-0.1wt% and pure PLLA decreased. The effect of

GNSs on α' form PLLA acts together with T_c on crystallization process, but it does not change the essence of the T_c effect on crystal formation. This implied that the effect of GNSs does not influence the essence of PLLA molecular chain mobility.

The shift of α' - α crystal formation transition of PLLA/GNSs-0.1wt% sample from that of pure PLLA sample to higher temperature can be interpreted. The acceleration effect of GNSs on the formation of α' form PLLA is more efficient than the formation of α form PLLA. At the same T_c s within α' - α crystal formation transition range, more α' form PLLA formation in PLLA/GNSs-0.1wt% formed than in pure PLLA. At T_c s higher but near the transition range, α' form PLLA formation in pure PLLA sample is too less to be detected, while in PLLA/GNSs-0.1wt% sample α' form PLLA content is increased due to the addition of GNSs. Thus, the α' - α crystal formation transition of PLLA in PLLA/GNSs-0.1wt% sample is shifted to higher temperature than that of pure PLLA sample.

With the kinetically formed α' crystal and thermodynamically form α crystal of PLLA in mind, it is of value to compare the effect of GNSs with the effects of PDLA and DBS. It can be proposed that GNSs could promote formation of α' crystal more than that of α crystal by enhancing the mobility of PLLA chain and thus accelerating α' crystal crystallization more. PDLA and DBS favor formation of α crystal because they could inhibit crystallization of α' crystal more than that of α crystal. All GNSs, PDLA and DBS play their roles by mainly affecting formation of α' crystal. This is why GNSs in PLLA resulted in a shift of α' - α crystal formation transition towards high temperatures, while it is inversely to PDLA or DBS. If one compares the effect of GNSs with that of melt shear on the crystal structure and crystallization rate of PLLA [5, 19], it can be concluded that both of them could accelerate nucleation of PLLA, but melt shear can't accelerate spherulite growth [19] while GNSs can increase both of the nucleation density and spherulite growth rate. This is because the influences of pre-ordered PLLA melt from melt shear are different from those influences of the increase of PLLA chain mobility on nucleation density and spherulite growth rate of PLLA, which also interpreted the shift of α' - α crystal formation transition towards high or low temperatures resulting from existence of GNSs or melt shear in PLLA, respectively.

4. Conclusions

Graphene Nanosheets (GNSs) are added into Poly(L-lactide) (PLLA) by solution blending and a PLLA/GNSs composite with GNSs content of 0.1wt% was obtained. The crystalline structures and crystallization behaviors of PLLA in PLLA/GNSs

composite were investigated and compared with those of pure PLLA. It was found that formation of α' form PLLA seems to be more preferred than that of α form PLLA in PLLA/GNSs at some T_c s due to the existence of GNSs, resulting in an observable shift of α' - α crystal formation transition region of PLLA to high T_c s in PLLA/GNSs comparing with that in pure PLLA. POM observations revealed that PLLA spherulites of α crystal were formed in PLLA/GNSs composite as well as in pure PLLA and the added GNSs can obviously accelerate the crystallization process of α form PLLA in PLLA/GNSs, including both the nucleation density and the spherulites growth rate u increased due to the increase of PLLA chains' mobility resulting from GNSs existence in PLLA and prior to steric hindrance of GNSs; whereas, GNSs seemed to have no observable influence on the zero growth temperature T_{zg} of PLLA which tends to be lower than the equilibrium melting point of PLLA. The SAXS results revealed that the long period L of PLLA in PLLA/GNSs composite are much smaller than those in pure PLLA, which can be interpreted successfully by Dual-lamellar stack model. Investigations on the melting behaviors of PLLA in both PLLA/GNSs and pure PLLA indicated that α' form PLLA in PLLA/GNSs composite isothermally crystallized at different T_c s within the temperature range of α' - α crystal formation transition region seems to be more perfect than those α' crystals in pure PLLA, while the α form PLLA in PLLA/GNSs seems to be less perfect than those α crystals in pure PLLA. The general T_c dependent behaviors of formation of α' form and α form PLLA in PLLA/GNSs were not changed and they were similar to those in pure PLLA.

Acknowledgement This work was supported by the National Natural Science Foundation of China (51173130, 21274149, and 21374077).

References:

- [1] Xiao P, Li H, Huang S, Wen H, Yu D, Shang Y, Li J, Wu Z, An L, Jiang S. *Cryst. Eng. Comm.* 2013; 15(39): 7914-7925.
- [2] Abe H, Kikkawa Y, Inoue Y, Doi Y. *Biomacromolecules* 2001; 2(3): 1007-1014.
- [3] Hoogsteen W, Postema A, Pennings A, Tenbrinke G, Zugenmaier P. *Macromolecules* 1990; 23(2): 634-642.
- [4] Pan P, Zhu B, Kai W, Dong T, Inoue Y. *Macromolecules* 2008; 41(12): 4296-4304.
- [5] Huang S, Li H, Jiang S, Chen X, An L. *Polymer* 2011; 52(15): 3478-3487.
- [6] Pan P, Liang Z, Zhu B, Dong T, Inoue Y. *Macromolecules* 2009; 42(9): 3374-3380.
- [7] Zhang J, Tashiro K, Tsuji H, Domb A. *Macromolecules* 2007; 40(4): 1049-1054.
- [8] Lai W. *J. Phys. Chem. B* 2011; 115(38): 11029-11037.

- [9] Kim I, Jeong Y. *J. Polym. Sci. Part B-Polym. Phys.* 2010; 48(8): 850-858.
- [10] Xu J, Chen T, Yang C, Li Z, Mao Y, Zeng B, Hsiao B. *Macromolecules* 2010; 43(11): 5000-5008.
- [11] Villmow T, Pötschke P, Pegel S, Häussler L, Kretzschmar B. *Polymer* 2008; 49(16): 3500-3509.
- [12] Kawai T, Rahman N, Matsuba G, Nishida K, Kanaya T, Nakano M, Okamoto H, Kawada J, Usuki A, Honma N, Nakajima K, Matsuda M. *Macromolecules* 2007; 40(26): 9463-9469.
- [13] Pan P, Kai W, Zhu B, Dong T, Inoue Y. *Macromolecules* 2007; 40(19): 6898-6905.
- [14] Zhang J, Tashiro K, Tsuji H, Domb A. *Macromolecules* 2008; 41(4): 1352-1357.
- [15] Zhang J, Duan Y, Sato H, Tsuji H, Noda I, Yan S, et al. *Macromolecules* 2005; 38(19): 8012-8021.
- [16] Zhang J, Tsuji H, Noda I, Ozaki Y. *Macromolecules* 2004; 37(17): 6433-6439.
- [17] Cartier L, Okihara T, Ikada Y, Tsuji H, Puiggali J, Lotz B. *Polymer* 2000; 41(25): 8909-8919.
- [18] Cho T, Strobl G. *Polymer* 2006; 47: 1036-1043.
- [19] Zhong Y, Fang H, Zhang Y, Wang Z, Yang J, Wang Z. *ACS Sustainable Chem. Eng.*, 2013; 1: 663-672
- [20] Allen M, Tung V, Kaner R. *Chem. Rev.* 2010; 110(1): 132-145.
- [21] Kim H, Abdala A, Macosko C. *Macromolecules* 2010; 43(16): 6515-6530.
- [22] Xu Z, Gao C. *Macromolecules* 2010; 43(16): 6716-6723.
- [23] Xu J, Chen C, Wang Y, Tang H, Li Z, Hsiao B. *Macromolecules* 2011; 44(8): 2808-2818.
- [24] Stankovich S, Dikin D, Dommett G, Kohlhaas K, Zimney E, Stach E, Piner R, Nguyen S, Ruoff R. *Nature* 2006; 442(7100): 282-286.
- [25] Kharchenko S, Douglas J, Obrzut J, Grulke E, Migler K. *Nature Materials* 2004; 3(8): 564-568.
- [26] Li L, Li B, Hood M, Li C. *Polymer* 2009; 50(4): 953-965.
- [27] Chen Y, Zhong G, Lei J, Li Z, Hsiao B. *Macromolecules* 2011; 44(20): 8080-8092.
- [28] Li L, Li C, Ni C. *J. Am. Chem. Soc.* 2006; 128(5): 1692-1699.
- [29] Patil N, Balzano L, Portale G, Rastogi S. *Carbon* 2010; 48(14): 4116-4128.
- [30] Garcia-Gutierrez MC, Hernandez JJ, Nogales A, Pantine P, Rueda DR, Ezquerro TA. *Macromolecules* 2008; 41(3): 844-851.

- [31] Hernandez J, Garcia-Gutierrez M, Nogales A, Rueda D, Ezquerro T. *Macromolecules* 2009; 42(13): 4374-4376.
- [32] Haggemueller R, Fischer J, Winey K. *Macromolecules* 2006; 39(8): 2964-2971.
- [33] Karatrantos A, Composto R, Winey K, Clarke N. *Macromolecules* 2011; 44(11): 4111-4119.
- [34] Xu D, Wang Z. *Polymer* 2008; 49(1): 330-338.
- [35] Rozanski A, Monasse B, Szkudlarek E, Pawlak A, Piorkowska E, Galeski A, et al. *Eur. Polym. J.* 2009; 45(1): 88-101.
- [36] Stribeck N, Zeinolebadi A, Sari M, Botta S, Jankova K, Hvilsted S, Drozdov A, Klitkou R, Potarniche C, Christiansen J, Ermini V. *Macromolecules* 2012; 45(2): 962-973.
- [37] Nowacki R, Monasse B, Piorkowska E, Galeski A, Haudin J. *Polymer* 2004; 45(14): 4877-4892.
- [38] Potts J, Murali S, Zhu Y, Zhao X, Ruoff R. *Macromolecules* 2011; 44(16): 6488-6495.
- [39] Wang H, Qiu Z. *Thermochim. Acta* 2011, 526(1-2): 229-236.
- [40] Chen H, Zhang W, Du X, Yang J, Zhang N, Huang T, Wang Y. *Thermochim. Acta* 2013; 566: 57-70.
- [41] Wurm A, Ismail M, Kretzschmar B, Pospiech D, Schick C. Retarded *Macromolecules* 2010; 43(3): 1480-1487.
- [42] Zhu P, Phillips A, Edward G. *J. Chem. Phys.* 2012; 136(5): 054903.
- [43] D'Haese M, Van Puyvelde P, Langouche F. *Macromolecules* 2010; 43(6): 2933-2941.
- [44] Li Y. *Polymer* 2011; 52(10): 2310-2318.
- [45] Zhu P, Tung J, Edward G, Nichols L. *J. Appl. Phys.* 2008; 103(12):124906-124914.
- [46] Nakagawa S, Kadana K, Ishizone T, Nojima S, Shimizu T, Yamaguchi K, Nakahama S. *Macromolecules* 2012; 45(10): 4120-4128.
- [47] Nojima S, Ohguma Y, Kadana K, Ishizone T, Iwasaki Y, Yamaguchi K. *Macromolecules* 2010; 43(8): 3916-3923.
- [48] Takenaka Y, Miyaji H, Hoshino A, Tracz A, Jeszka J K, Kucinska I. *Macromolecules* 2004; 37(26): 9667-9669.
- [49] Yang J, Lin S, Lee Y. *J. Mater. Chem.* 2012; 22: 10805-10815.
- [50] Wang H, Qiu Z. *Thermochim. Acta* 2012, 527: 40-46.
- [51] Cho T, Stille W, Strobl G. *Colloid. Polym. Sci.* 2007; 285: 931-934.

- [52] Strobl G, Cho T Y. *Eur. Phys. J. E* 2007; 23: 55-65
- [53] Wen H, Jiang S, Men Y, Zhang X, An L, Wu Z. *J. Chem. Phys.* 2009; 130(16): 164909.
- [54] Kobayashi J, Asahi T, Ichiki M, Okikawa A, Suzuki H, Watanabe T, Fukuda E, Shikinami Y. *J. Appl. Phys.* 1995; 77: 2957-2973.
- [55] Marega C, Marigo A, Di Noto V, Zannetti R. *Makromol. Chem.* 1992; 193: 1599-1606.
- [56] Zhang J, Tashiro K, Domb A, Tsuji H. *Macromol. Symp.* 2006; 242(1): 274-278.
- [57] Ohtani Y, Okumura K, Kawaguchi K. *J. Macromol. Sci. Phys.* 2003; 42(3-4): 875-888.
- [58] Dikovsky D, Marom G, Avila-Orta C, Somani R, Hsiao B. *Polymer* 2005; 46: 3096-3104.
- [59] Patti A. *J. Phys. Chem. B* 2014; 118: 3731-3742
- [60] Xiao H, Lu W, Yeh J. *J. Appl. Polym. Sci.*, 2009; 113: 112-121.
- [61] Tsuji H., Miyauchi S. *Polym. Degrad. Stab.*, 2001; 71: 415-424.
- [62] Chu B, Hsiao B. *Chem. Rev.* 2001; 101(6): 1727-1762.